Experimental and Numerical Modeling of the Extrusion Process in 1050A Aluminum Alloy for Design of Impact Energy-Absorbing Devices

G. Ryzińska[a] and R. Gieleta[b]

[a] Rzeszów University of Technology, Rzeszów, Poland

[b] Military University of Technology, Warsaw, Poland

The results obtained experimentally with the use of Hopkinson bar and numerical results on backward extrusion of 1050A aluminum at 10 m/s tool speed are presented, in order to assess the extrusion technology applied in the design of energy-absorbing devices. The devices of this type should satisfy the requirements, particularly, constant force versus displacement of the piston and the amount of the energy absorbed by the object. Numerical analyses of three variants of the absorbing device geometry were presented. The obtained results allowed an appropriate selection of geometric parameters of the device, and, as a result, the requirement of the proper amount of absorbed energy was satisfied.

Keywords: extrusion, 1050A aluminum alloy, finite element method (FEM), Hopkinson bar.

Introduction. The increasing competition and intensification of production in the engineering industry make it necessary to introduce new materials with desired properties, as well as to search for new unconventional applications of previously known technologies of metal forming, e.g., extrusion. One of such innovations is an attempt to apply the elements of extrusion technology in the design of devices absorbing the impact energy. When designing this type of solutions, the detailed information on the behavior of a metallic material applied in the range of high-speed deformations up to 5000 s^{-1} is necessary. There are mathematical models pertmitting description of the behavior of material subjected to deformation with a very high speed. However, noteworthy is that these models require the determination of a number of constants and coefficients for each material [1–3]. The alternative solution is to use the data on the material behavior material in the range of high-speed deformations obtained by using the advanced research equipment. The most commonly used method for determining material properties at high strain rates is the split-Hopkinson pressure test [4–9]. There is also a method with use of a rotary hammer, which allows stretching and bending of the specimens with linear velocity ranged from 5 to 40 m/s, which is equal to strain rate ranged from 10^2 to 10^4 s^{-1} [10]. The critical issue of the research on dynamic deformation, also conducted on flywheel machines, is the course and the interpretation of the achieved performance graph. There are many doubts as to the correctness of the analysis of the results, especially at the starting phase of deformation. Whether the observed varied performance graphs are caused by the specific design and work of the dynamic deformation of the research device, the structure of the gripper/handle, the specimen shape and the ability to identify and tune-off/filter the interferences [11, 12].

In this paper, the test results obtained with an application of the Hopkinson bar and numerical calculation results of backward extrusion process of 1050A aluminum grade at a speed of 10 m/s are presented. The elements of extrusion technology have been used in the process of designing of the impact energy absorbing device.

Currently used technology of the controlled acquisition and absorption of impact energy consists mainly of two types: crash technology and technology of springs. The crash technology, innovative and patented by Axtone company, is based upon a permanent plastic

deformation of metal filament sheared from the outer surface of the bumper body (including peeling and folding technology). Upon the collision, the outer surface of the bumper is machined by the cutting blades. The level of absorbed energy depends on the size and the cross section of the cutting tape, which makes possible a rather wide range of control parameters of the device, depending on the needs of the particular application. The crash bumpers, currently produced in accordance with the applicable standards, guarantee a controlled acquisition of large amounts of energy emerging as a result of a collision, in case of emergency situations. Energy absorption capacity of a bumper often reaches 1300 kJ. For comparison, the currently used standard bumper can absorb about 70 kJ [13]. The key aspect of all safety systems is their reliability. This applies to all bumpers, whose efficiency must be confirmed by a number of full-scale tests. Crash technology is based on a controlled takeover and absorption of a very high energy under the conditions of the accident taking place at high speeds. To ensure the maximum flexibility of the proposed solutions, the individual solutions, in accordance with the diverse needs of customers, are currently being designed based on the patented cutting technology . In view of the increasing competition, there is a search for new solutions in this field, which can expand the range of products offered and introduce a better performance of these products. This concerns the quantity of energy absorption, stability or strength during operation. The devices for absorbing impact energy must meet certain requirements, such as the amount of energy absorbed, a stable force level during an operation, a certain value of force, etc. When analyzing the requirements for such devices, it is noteworthy that, in the case of a test of an application of extrusion technology, the condition of a constant force can be met by the backward extrusion technology.

A very important issue is the choice of the charge material, which, while deforming, allows one to absorb the stored energy. Due to the low propensity to strengthening and low weight, the aluminum alloys have been taken into account (Table 1), from which the available 1050A aluminum alloy has been chosen.

T a b l e 1
Properties of the Selected Low Strain Hardening Materials [14]

PN EN 573-3	Chemical composition (%)	$R_{0.2}$, MPa	R_m, MPa
1080A	99.8Al	15–105	60–150
1070A	99.7Al	15–105	60–150
1050A	99.5Al	20–130	65–160
1200	99.0Al	25–140	75–170
1100	99.0Al	105	110

Material Test. In order to obtain data on the material behavior for a wide range of strain rate, the static compression tests and dynamic tests using the Hopkinson bar have been performed. Static compression tests of aluminum alloy have been carried out on the Instron 8862 testing machine. The test specimens in the form of cylinders of dimensions $D = 10$ mm and $L = 7.5$ mm have been prepared by turning (Fig. 1).

Compression tests have been carried out with controlling of the displacement motion of the jaws at a rate of 5 mm/min. For an accurate measurement of specimen contraction/ shortening, the Instron extensometer attached directly to the compression pads has been used. The static compression test procedure is illustrated by Fig. 2.
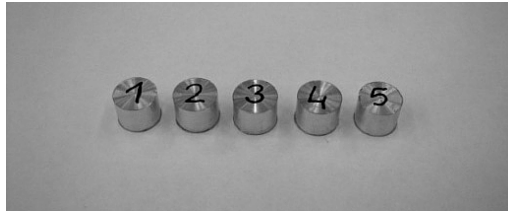
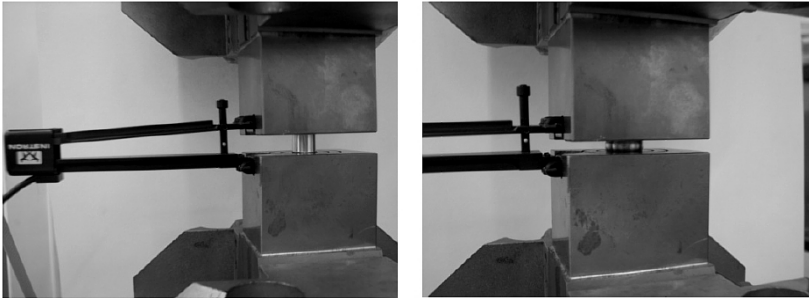Fig. 1. 1050A aluminum alloy specimens before compression test.

Fig. 2. Static compression tests of 1050A aluminum alloy.

In the static compression tests, the relations of stresses and strains have been determined. Overall figures obtained in tests of static compression of the aluminum alloy have been presented in Fig. 3. The graph shows the engineering stresses and strains. The shapes of specimens after the tests are also shown in Fig. 3.
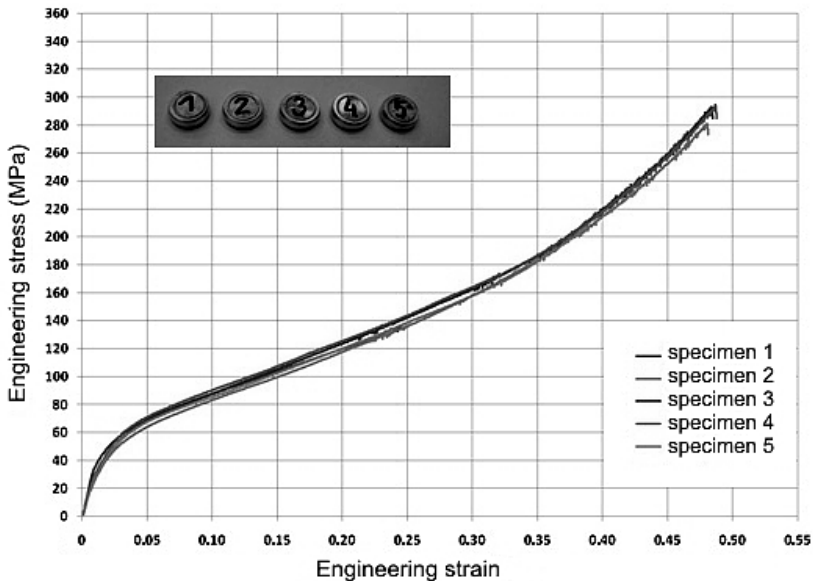

Fig. 3. Collective graph of 1050A aluminum alloy static compression test and shapes of specimens after static compression test.

Compression tests at high strain rate have been carried out in a specialized test bench with a system of elastic rods (modified Hopkinson bar or the Kolsky bar). A striker bar of specified length produces an adequate loading duration. The impact of the striker bar triggers

the automatic data registration from the strain gauges located on both the incident and transmission bars. Stress, strain, and strain rate are then calculated from the data collected via the strain gauges. A general schematic representation of the equipment is shown in Fig. 4. For the signal amplification from the measuring rods (electroresistant deformeter) and the signal acquisition from the bench (the signals from the laser barriers for measuring the projectile velocity) the fast processes amplifier LTT500 by Tasler (LTT Labortechnik GmbH Tasler, Germany), the measuring card NI USB-6366 by National Instruments and the originally developed specialized software have been applied. In the described bench, the amplifier and the A/D measuring card have a bandwidth equal to 1 MHz. During the test the signals have been sampled at the time interval of 0.5 μs.

A typical specimen inserted between measuring bars is depicted in Fig. 5, while samples of waveforms of the measuring rods are shown in Figs. 6 and 7.
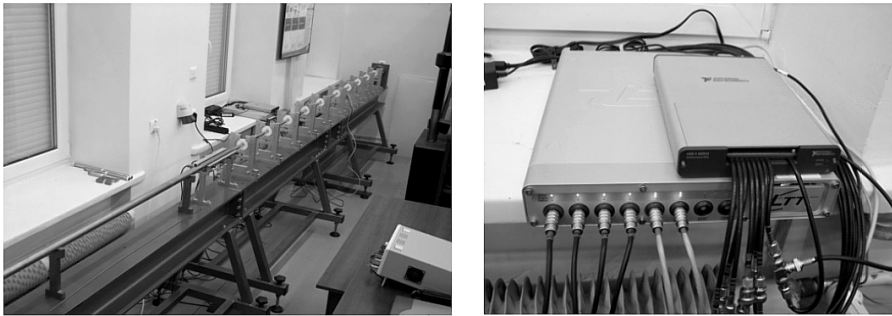

Fig. 4. A perspective view of the SHPB apparatus for testing materials at high strain rates (SHPB = split-Hopkinson pressure bar).
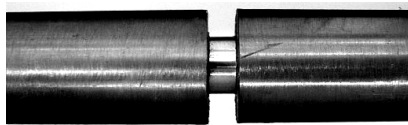

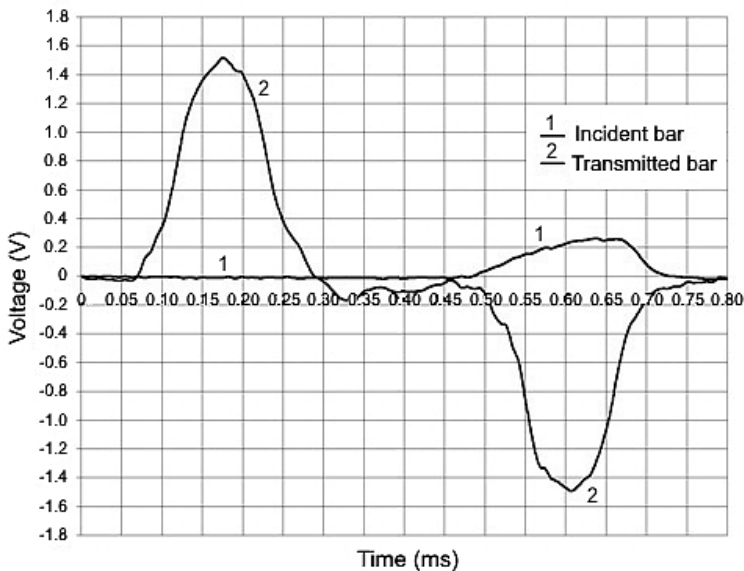Fig. 5. Specimen between the measuring bars.

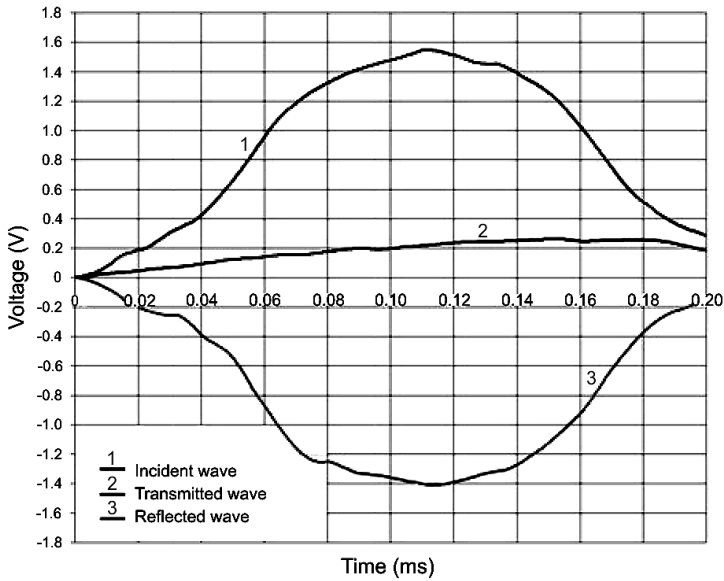Fig. 6. Exemplary signals from the measuring bars.

Fig. 7. Signals from measuring bars processed for calculations of stresses and strains.

On the basis of the registered signals from the measuring rods, the calculations of strains, stresses and strain rates in a specimen have been performed according to the following relationships for the elastic rods:

$$\varepsilon(t) = -2\frac{C_0}{L}\int_0^t \varepsilon_R(t)dt, \tag{1}$$

$$\sigma(t) = \frac{ES_{p0}}{S_{pr}}\varepsilon_T(t), \tag{2}$$

$$\dot{\varepsilon}(t) = -2\frac{C_0}{L}\varepsilon_R(t), \tag{3}$$

where C_0 is wave propagation velocity, L is length of the specimen, E is the Young modulus of measuring bars, S_{p0} and S_{pr} are cross-sectional areas of bar and specimen, respectively, $\varepsilon_R(t)$ and $\varepsilon_T(t)$ are signals in time for the reflected wave and the wave in transmitted bar, respectively.

The calculated values of $\varepsilon(t)$ and $\sigma(t)$ were used to construct plot of the stresses and strains for the given strain rate.

The overall graphs obtained in the compression tests at high strain rates are shown in Figs. 8–10. Figure 11 shows an example of the specimens after the dynamic tests.

Comparing the relationship between stresses and strains for different strain rates, it can be seen that the tested 1050A aluminum alloy shows a small sensitivity to the strain rate. The maximum stress at a strain of 0.3 for the specimen type D10/L5 is equal to 180 MPa, for the specimen type D10/L3 at the same deformation is 220 MPa, and for the specimen type D10/L1 is 270 MPa.

The data obtained from the static compression tests and from the tests with an application of the Hopkinson bar have been applied for simulation of the material behavior in the backward extrusion process at high speed.
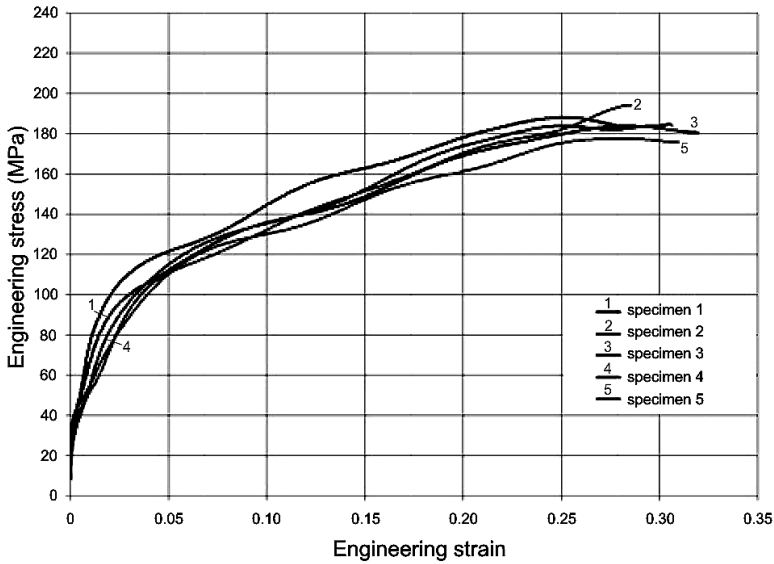
Fig. 8. Collective graph of 1050A aluminum alloy (compression test at high strain rates) D10/L5.
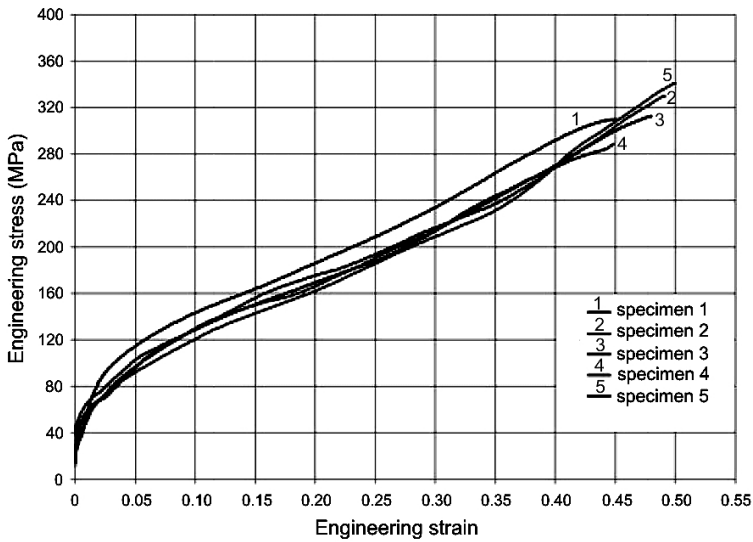

Fig. 9. Collective graph of 1050A aluminum alloy (compression test at high strain rates) D10/L3.

FEM Modeling. In the calculations of the impact energy absorption device, the SimufactForming software has been used [15]. The geometry of the model has been set as axisymmetric. It has been assumed that the deformable aluminum alloy charge closed in a rigid container gets into a contact with a rigid punch. Application of the feedstock in the form of a sleeve ensures that the total deformable material remains in the container (Fig. 12c). Motion of the punch has been forced by a single stroke with a suitably chosen large initial mass (20 ton) of the linear speed of 10 m/s. The dimensions of the aluminum alloy charge, in all cases, have been established, and in the case of the punch three different variants of outer diameter ($d_1 = 100$ mm, $d_2 = 102$ mm, and $d_3 = 104$ mm) have been applied (Fig. 12). In numerical calculations, elements of Quad 10 type of 0.5 mm size were used. A detailed description of the FEM model is given in Table 2.
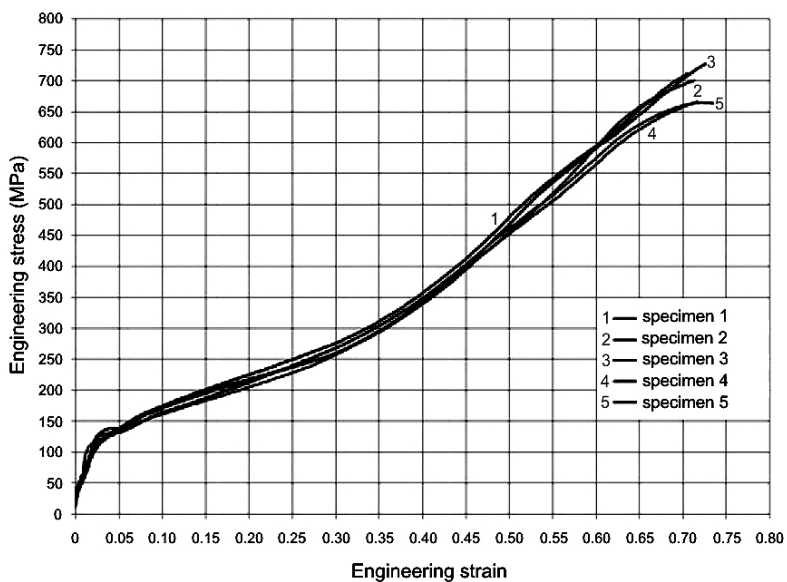
Fig. 10. Collective graph of 1050A aluminum (compression test at high strain rates) D10/L1.

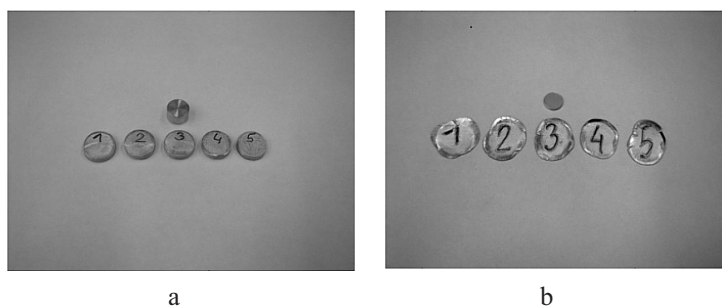a   b

Fig. 11. Exemplary specimens of 1050A aluminum after dynamic compression test at high strain rates: (a) $D = 10$ mm, $L = 5$ mm; (b) $D = 10$ mm, $L = 1$ mm.
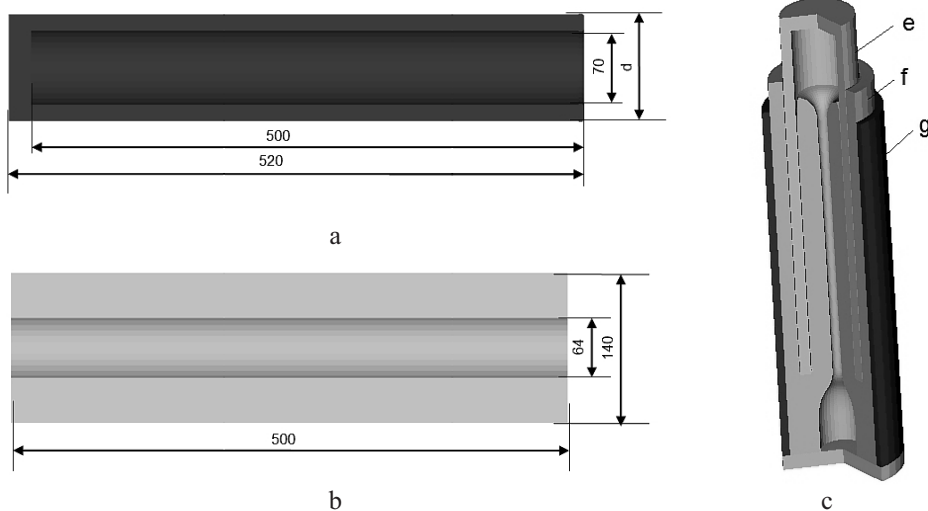

a

b   c

Fig. 12. Geometrical parameters of the impact energy-absorbing device: (a) punch; (b) ingot; (c) general view (e – punch, f – ingot, g – container).

T a b l e 2

Selected Features of the Applied FEM Model

Feature	Description
Type of geometry	Axisymmetric
Approach	Updated Lagrangian
Friction	Bilinear (Coulomb 0.05 and Tresca 0.08)
Temperature	293 K
Initial velocity	10 m/s
Mass of hammer	20 ton
Expected value of absorbed energy	1 MJ
Expected force	2000 kN
Number of elements	2384
Type of element	Quad 10
Remeshing	Yes
Integration procedure	Explicit
Yield criterion	Huber–Mises
Flow rule	Prandtl–Reuss

Based on the calculations, the graphs of the relations of the force from the punch displacement for three cases of the punch geometry have been constructed. Depending on the dimensions, three different values of the maximum force have been obtained (Fig. 13).
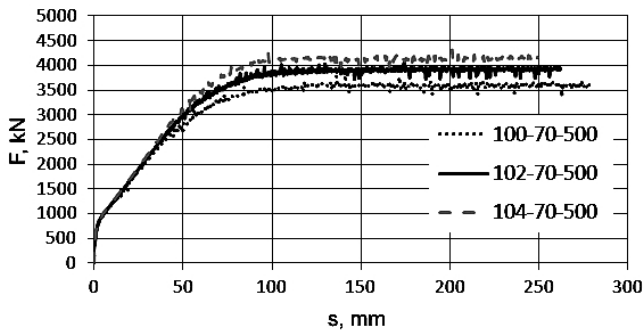

Fig. 13. The relationship between force and displacement for the examined geometric variants of punch (1050A aluminum).

The varied size of the resulting force depending on the geometry of the applied punch is related to the time, in which the impact energy is absorbed, and the time of deceleration in the tool from 10 to 0 m/s (Figs. 14 and 15). Exemplary results of FEM calculations (effective plastic strain and effective stress in ingot) are shown in Fig. 16.

The relations obtained with an application of three different geometric configurations of the punch make it possible to assess the extent, to which the device is able to absorb the necessary amount of energy by the controlled deformation of the 1050A aluminum. This is due to the time required to slow down the motion of the punch. The calculation results show that the use of an external diameter of the punch of 104 mm can meet the requirement
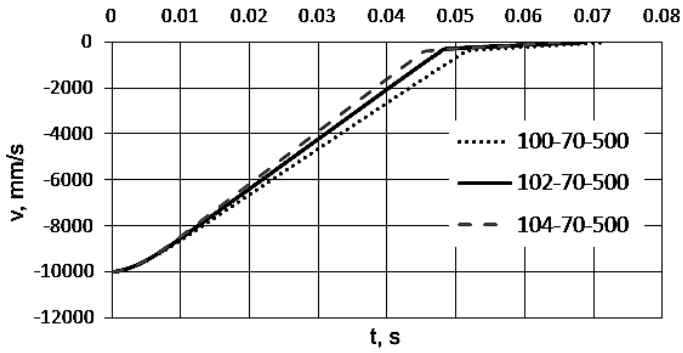
Fig. 14. Dependence between time and punch velocity for various geometric punch configurations (1050A aluminum).
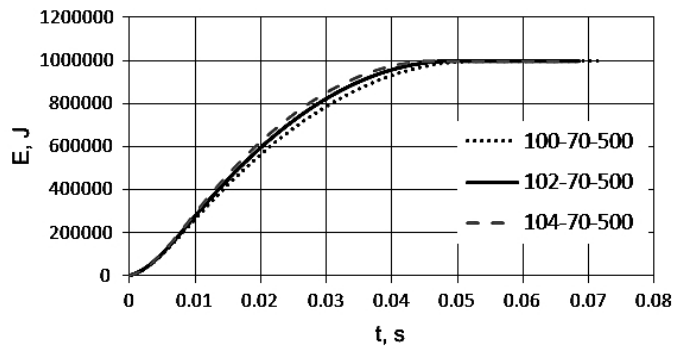

Fig. 15. Dependence between time and absorbed energy for various geometric punch configurations (1050A aluminum).
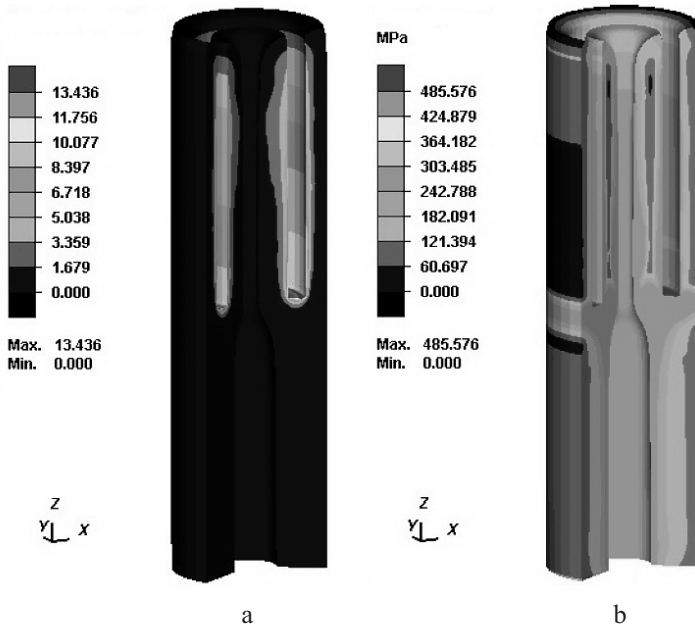

Fig. 16. Exemplary results of FEM calculations: (a) effective plastic strain – ingot 102-70-500; (b) effective stress – ingot 102-70-500.

to absorb 1 MJ of energy in the shortest possible time. In the transport industries, there is a need for devices absorbing different preset amounts of the impact energy, which vary with the particular vehicle wight. That is why an ability to change parameters of operation of such a device is very important and it can be achieved by variation of the punch geometry. At the next phase, it is planned to test the prototype of the designed device.

Conclusions. In this paper, the results of experimental research performed with an application of the Hopkinson bar and of numerical calculations of backward extrusion process of 1050A aluminum at a speed of 10 m/s have been presented. Extrusion technology have been used in designing of the impact energy absorbing device. The analysis of results obtained made it possible to draw the following conclusions:

1. The research performed confirmed a possibility to use the extrusion technology in the design of the impact energy-absorbing devices.

2. On the basis of calculations it can be stated that the process of backward 1050A aluminum extrusion can be used in the construction of the impact energy-absorbing devices, while detailed results of the calculations should be confirmed experimentally.

3. Calculations have shown that the use of geometrical parameters of punch 100-70-500 makes it possible to completely absorb 1 MJ of impact energy during the time of 0.072 s. Increase in the punch cross-sectional area results in shortening the time required to absorb the impact energy and to increase the force.

4. The solution satisfies the industrial requirements of the constant force, while the ability to absorb a certain amount of energy turned out to be higher than in the existing solutions, which can be used, in particular, in rail vehicles with a high weight. Application of the feedstock in the form of a sleeve allows one to keep the total deformable material in the container, in contrast to the existing crash bumper solutions.

5. A significant advantage of this solution is a possibility of continuous adjustment of the force, as well as of the amount of energy absorbed, depending on the weight of the vehicle, by a suitable choice of the device geometry, which it is advantageous for industrial production. The developed impact energy-absorbing device may widen the scope of manufacturers of this type of equipment on the market.

1. S. R. Bodner and Y. Partom, "Constitutive equations for elastic-viscoplastic strain-hardening materials," *J. Appl. Mech.*, **42**, No. 2, 385–389 (1975).

2. S. Huang and A. S. Khan, "Modeling the mechanical behavior of 1100-0 aluminum at different strain rates by the Bodner–Partom model," *Int. J. Plasticity*, **8**, 501–517 (1992).

3. J. Bocko, V. Nohajova, and J. Šarloši, "Simulation of material behaviour by Bodner–Partom model," *Am. J. Mech. Eng.*, **3**, No. 6, 181–185 (2015).

4. T. Jankowiak, A. Rusinek, and T. Łodygowski, "Validation of the Klepaczko–Malinowski model for friction correction and recommendations on split Hopkinson pressure bar," *Finite Elem. Anal. Des.*, **47**, No. 10, 1191–1208 (2011).

5. G. I. Mylonas, G. N. Labeas, and Sp. G. Pantelakis, "High strain rate behaviour of aluminium alloys using split Hopkinson bar (Shb) testing," in: E. E. Gdoutos (Ed.), *Experimental Analysis of Nano and Engineering Materials and Structures* (Proc. of the 13th Int. Conf. on Experimental Mechanics, July 1–6, 2007, Alexandroupolis, Greece), Springer (2007), pp. 161–162.

6. J. Rodriguez, R. Cortés, M. A. Martinez, et al., "Numerical study of the specimen size effect in the split Hopkinson pressure bar tests," *J. Mater. Sci.*, **30**, 4720–4725 (1995).

7. J. R. Klepaczko and G. C. Y. Chiem, "On rate sensitivity of FCC metals, instantaneous rate sensitivity and rate sensitivity of strain hardening," *J. Mech. Phys. Solids*, **34**, 29–54 (1986).

8. Stepanov G. V. and V. I. Zubov, "Generalized deformation curve for high-strength steel over a wide range of strain rates," *Strength Mater.*, **36**, No. 2, 165–170 (2004).

9. J. D. Seidt, J. Michael Pereira, and A. Gilat, "Influence of fabrication method on tensile response of split Hopkinson bar-sized specimens," *J. Test. Eval.*, **43**, No. 6, 1563–1573 (2015).

10. J. Pawlicki, K. Rodak, and A. Płachta, "Plasticity of selected metallic materials in dynamic deformation conditions," *Politechnika Śląska*, Ser. *Transport*, **83**, 173–182 (2014).

11. C. Wong, *IISI–AutoCo Round–Robin Dynamic Tensile Testing Project*, International Iron and Steel Institute (2005).

12. A. Niechajowicz and A. Tobota, "Application of flywheel machine for sheet metal dynamic tensile tests," *Arch. Civ. Mech. Eng.*, **8**, No. 2, 129–137 (2008).

13. http://www.axtone.eu (2016).

14. http://www.sebros.eu/aluminium/

15. Simufact.Forming v.13.2.